

目次

基于机器学习的珠三角秋季臭氧浓度预测 陈镇, 刘润, 罗征, 薛鑫, 汪瑶, 赵志军 (1)

粤港澳大湾区大气PM_{2.5}浓度的遥感估算模型 代园园, 龚绍琦, 张存杰, 闵爱莲, 王海君 (8)

典型输送通道城市冬季PM_{2.5}污染与传输变化特征 代武俊, 周颖, 王晓琦, 齐鹏 (23)

郑州市夏季PM_{2.5}中二次无机组分污染特征及其影响因素 和兵, 杨洁茹, 徐艺斐, 袁明浩, 翟诗婷, 赵长民, 王申博, 张瑞芹 (36)

重庆典型城区冬季碳质气溶胶的污染特征及来源解析 彭超, 李振亮, 向英, 王晓宸, 汪凌韬, 张晟, 翟崇治, 陈阳, 杨复沫, 翟天宇 (48)

2022年8月成渝两地臭氧污染差异影响因素分析 陈木兰, 李振亮, 彭超, 邓也, 宋丹林, 谭钦文 (61)

2020年“三连击”台风对我国东部地区O₃污染的影响分析 花丛, 尤媛, 王晴, 张碧辉 (71)

北京城区夏季VOCs初始体积分数特征及来源解析 张博韬, 景宽, 王琴, 安欣欣, 鹿海峰, 王陈婧, 王友峰, 刘保献 (81)

机动车减排降碳综合评价体系综述 范朝阳, 佟惠, 梁晓宇, 彭剑飞 (93)

基于LEAP模型的长三角某市碳达峰情景 杨峰, 张贵驰, 孙伟, 谢放尖, 揣小伟, 孙瑞玲 (104)

广东省船舶二氧化碳排放驱动因素与减排潜力 翁淑娟, 刘颖颖, 唐凤, 沙青娥, 彭勃, 王焯嘉, 陈诚, 张雪驰, 李京洁, 陈豪琪, 郑君瑜, 宋献中 (115)

给水厂典型工艺碳排放特征与影响因素 张翔宇, 胡建坤, 马凯, 高欣慰, 魏月华, 韩宏大, 李克勋 (123)

中国饮用水中砷的分布特征及基于伤残调整寿命年的健康风险评估 襄殿程, 齐媛, 肖淑敏, 苏高新, 郭宇新 (131)

太湖水体和沉积物中有机磷酸酯的时空分布和风险评估 张成诺, 钟琴, 栾博文, 周涛, 顾帆, 李伟飞, 邹华 (140)

水产养殖环境中农兽药物的污染暴露水平及其风险影响评价 张楷文, 张海燕, 孔聪, 顾润润, 田良良, 杨光昕, 王媛, 陈冈, 沈晓盛 (151)

长江朱沱断面磷浓度与通量变化及来源解析 姜保峰, 谢卫民, 黄波, 刘旻璇 (159)

珠江河口地表水锰氧化物对磷的“载-卸”作用 李睿, 梁作兵, 伍祺瑞, 杨晨晨, 田帝, 高磊, 陈建耀 (173)

富春江水库浮游植物功能群变化的成因 张萍, 王炜, 朱梦圆, 国超旋, 邹伟, 许海, 朱广伟 (181)

合浦盆地西部地区地下水水化学特征及形成机制 陈雯, 吴亚, 张宏鑫, 刘怀庆 (194)

新疆车尔臣河流域绿洲带地下水咸化与污染主控因素 李军, 欧阳宏涛, 周金龙 (207)

京津冀地区生态系统健康时空演变及其影响因素 李魁明, 王晓燕, 姚罗兰 (218)

近30年辽河三角洲生态系统服务价值时空演变及影响因素分析 王耕, 张芙蓉 (228)

光伏电站建设对陆地生态环境的影响: 研究进展与展望 田政卿, 张勇, 刘向, 陈生云, 柳本立, 吴纪华 (239)

大兴安岭林草交错带植被NDVI时空演变及定量归因 石淞, 李文, 曲琛, 杨子仪 (248)

西南地区不同类型植被NPP时空演变及影响因素探究 徐勇, 郑志威, 孟禹弛, 盘钰春, 郭振东, 张炎 (262)

不同海拔梯度下极端气候事件对松花江流域植被NPP的影响 崔嵩, 贾朝阳, 郭亮, 付强, 刘东 (275)

基于InVEST与CA-Markov模型的昆明市碳储量时空演变与预测 帕茹克·吾斯曼江, 艾东, 方一舒, 张益宾, 李牧, 郝晋珉 (287)

基于PLUS-InVEST模型的酒泉市生态系统碳储量时空演变与预测 石晶, 石培基, 王梓洋, 程番苑 (300)

长江下游沿江平原土壤发育过程中碳库分配动态 胡丹阳, 张欢, 宿宝巍, 张娅璐, 王永宏, 纪佳辰, 杨浩, 高超 (314)

漓江流域喀斯特森林土壤有机碳空间分布格局及其驱动因子 申楷慧, 魏识广, 李林, 储小雪, 钟建军, 周景钢, 赵毅 (323)

不同土地利用方式对岩溶区土壤有机碳组分稳定性的影响 陈坚淇, 贾亚男, 贺秋芳, 江可, 陈畅, 叶凯 (335)

紫色土丘陵区坡地柑橘园土壤碳氮的空间分布特征 李子阳, 陈露, 赵鹏, 周明华, 郑静, 朱波 (343)

氮添加与凋落物处理对橡胶林砖红壤有机碳组分及酶活性的影响 薛欣欣, 任常琦, 罗雪华, 王文斌, 赵春梅, 张永发 (354)

重庆化肥投入驱动因素、减量潜力及环境效应分析 梁涛, 赵敬坤, 李红梅, 王妍, 曹中华, 张务帅, 王孝忠, 郭超仪, 石孝均, 陈新平 (364)

中国土壤中全氟和多氟烷基物质的分布、迁移及管控研究进展 刘浩然, 邢静怡, 任文杰 (376)

基于多源辅助变量和随机森林模型的耕地土壤重金属含量空间分布预测 解雪峰, 郭炜炜, 濮励杰, 缪源卿, 蒋国俊, 张建珍, 徐飞, 吴涛 (386)

基于源导向的农用地土壤重金属健康风险评估及优先控制因子分析 马杰, 葛森, 王胜蓝, 邓力, 孙静, 蒋月, 周林 (396)

铜陵某废弃硫铁矿矿区土壤重金属污染特征及来源解析 李如忠, 刘宇昊, 黄言欢, 吴鸿飞 (407)

天水市主城区公交站地表灰尘重金属来源解析及污染评价 李春艳, 王新民, 王海, 吕晓斌 (417)

基于大田试验的土壤-水稻镉对不同调理剂的响应 唐乐斌, 刘新彩, 宋波, 马丽钧, 黄凤艳 (429)

腐殖质活性组分对土壤镉有效性的调控效应与水稻安全临界阈值 胡秀芝, 宋毅, 王天雨, 蒋珍茂, 魏世强 (439)

生物质炭与铁钙材料对镉砷复合污染农田土壤的修复 吴秋产, 吴骥子, 赵科理, 连斌, 袁峰, 孙洪, 田欣 (450)

人体微塑料污染特征及健康风险研究进展 马敏东, 赵洋尘, 朱龙, 王伟平, 康玉麟, 安立会 (459)

聚苯乙烯微塑料联合镉污染对土壤理化性质和生菜(*Lactuca sativa*)生理生态的影响 牛佳瑞, 邹勇军, 简敏菲, 黄楚红, 李金燕, 穆霆, 刘淑丽 (470)

转录组分析植物促生细菌缓解高粱微塑料和重金属复合污染胁迫机制 刘泳岐, 赵超禹, 任学敏, 李玉英, 张英君, 张浩, 韩辉, 陈兆进 (480)

微塑料对土壤中养分和镉淋失的影响 赵群芳, 褚龙威, 丁原红, 王发园 (489)

微塑料和非对土壤化学性质、酶活性及微生物群落的影响 刘沙沙, 秦建桥, 吴贤格 (496)

民勤荒漠绿洲过渡带人工梭梭林土壤细菌群落结构及功能预测 王安林, 马瑞, 马彦军, 吕彦勋 (508)

不同灌溉水盐度下土壤真菌群落对生物炭施用的响应 郑志玉, 郭晓雯, 闵伟 (520)

厨余垃圾有机肥对土壤微生物活性及功能的影响 刘美灵, 汪益民, 金文豪, 王永冉, 王嘉和, 柴一博, 彭丽媛, 秦华 (530)

土壤真菌群落结构对辣椒长期连作的响应特征 陈芬, 余高, 王谢丰, 李廷亮, 孙约兵 (543)

叶面喷施硅肥对再生水灌溉水稻叶际细菌群落结构及功能基因的影响 梁胜贤, 刘春成, 胡超, 崔二苹, 李中阳, 樊向阳, 崔丙健 (555)

昌黎县海域细菌群落和抗生素抗性基因分析 王秋水, 程波, 刘悦, 邓婕, 徐岩, 孙朝徽, 袁立艳, 左嘉, 司飞, 高丽娟 (567)

基于高通量定量PCR与高通量测序技术研究城市湿地公园抗生素抗性基因污染特征 黄福义, 周曙屹, 潘婷, 周昕原, 苏建强, 张娴 (576)

城区第四系沉积柱中抗生素的垂向分布特征及环境影响因素 刘可, 童蕾, 甘翠, 王逸文, 张嘉越, 何军 (584)

氢氧化钾改性玉米秸秆生物炭对水中土霉素的吸附特性及机制 刘总堂, 孙玉凤, 费正皓, 沙新龙, 温小菊, 钱彬彬, 陈建, 谷成刚 (594)

CO₂气氛热解与硝酸改性的生物炭Pb²⁺吸附性能对比 江豪, 陈瑞芝, 朱自洋, 王琳, 段文斌, 陈芳媛 (606)

《环境科学》征订启事(70) 《环境科学》征稿简则(193) 信息(334,554,605)

珠江河口地表水锰氧化物对磷的“载-卸”作用

李睿^{1,2}, 梁作兵¹, 伍祺瑞¹, 杨晨晨¹, 田帝¹, 高磊^{2*}, 陈建耀^{1*}

(1. 中山大学地理科学与规划学院, 广州 510275; 2. 中国科学院华南植物园退化生态系统植被恢复与管理重点实验室, 广州 510650)

摘要: 地表径流输送的磷在河口水环境营养结构平衡和初级生产力调节中起到了关键作用. 通过测定不同季节珠江下游及河口地表水阴阳离子、总磷及其形态、颗粒态铁(PFe)、颗粒态锰(PMn)和颗粒态铝(PAl)等理化性质, 探究咸-淡水交互区内磷的时空分布特征, 并识别控制磷迁移转化的关键因素. 结果表明, $\rho(\text{TP})$ (28.88 ~ 233.68 $\mu\text{g}\cdot\text{L}^{-1}$) 受到沉降和稀释作用随盐度升高呈下降趋势, 且占比大小为: 溶解态无机磷(DIP, 37.3%) > 颗粒态无机磷(PIP, 22.7%) > 溶解态有机磷(DOP, 21.0%) > 颗粒态有机磷(POP, 19.0%). PIP与PFe、PMn和PAl有显著($P < 0.05$)的共迁移相关关系, 水体盐度的升高促进了悬浮颗粒态无机磷的解吸, 且该过程主要发生在咸-淡水界面附近. 无机磷的固-液分配系数(K_d)与盐度间的显著正相关关系($P < 0.001$)表明, 高盐度水域PIP主要以更稳定的结合形态存在. K_d 与PMn的显著正相关关系($P < 0.01$)证明了Mn氧化物对磷的“载-卸”作用: 从淡水环境中吸附携带无机磷, 迁移至高盐度水体释放.

关键词: 咸-淡水交互区; 盐度梯度; 磷; 赋存形态; 迁移转化

中图分类号: X142 文献标识码: A 文章编号: 0250-3301(2024)01-0173-08 DOI: 10.13227/j.hjx.202301010

“Load-Unload” Effect of Manganese Oxides on Phosphorus in Surface Water of the Pearl River Estuary

LI Rui^{1,2}, LIANG Zuo-bing¹, WU Qi-ru¹, YANG Chen-chen¹, TIAN Di¹, GAO Lei^{2*}, CHEN Jian-yao^{1*}

(1. School of Geography and Planning, Sun Yat-sen University, Guangzhou 510275, China; 2. Key Laboratory of Vegetation Restoration and Management of Degraded Ecosystems, South China Botanical Garden, Chinese Academy of Sciences, Guangzhou 510650, China)

Abstract: Phosphorus (P) conveyed by surface runoff plays an essential role in regulating nutrient balance and primary production in estuarine waters. In this study, basic physicochemical properties, total phosphorus (TP, including speciation), particulate iron (PFe), particulate manganese (PMn), and particulate aluminum (PAl) of the surface water in the Pearl River Estuary (PRE) in different seasons were determined to investigate the spatiotemporal distribution characteristics of P and to identify the crucial factor controlling P migration and transformation in the freshwater-saltwater interaction zone. TP concentrations (28.88-233.68 $\mu\text{g}\cdot\text{L}^{-1}$) decreased with increasing salinity gradient owing to deposition and dilution. The proportions of P speciation followed a decreasing order as dissolved inorganic phosphorus (DIP, 37.3%) > particulate inorganic phosphorus (PIP, 22.7%) > dissolved organic phosphorus (DOP, 21.0%) > particulate organic phosphorus (POP, 19.0%). PIP was positively related to PFe, PMn, and PAl ($P < 0.05$), confirming their concurrent migration behaviors. In addition, the increase in salinity promoted the desorption of phosphate on the suspended particulate matters, which mainly took place near the freshwater-saltwater interface. A significant positive correlation ($P < 0.001$) between the solid-liquid phase partitioning coefficient (K_d) of phosphate and salinity indicated that PIP was present mainly in more stable forms in the brackish water. Most importantly, a better relationship between K_d and PMn ($P < 0.01$) supported our scientific hypothesis of the “load-unload” effect of Mn oxides on P: particulate-carrying phosphates transported from the freshwater zone tend to be desorbed and released into the brackish water.

Key words: freshwater-saltwater interaction zone; salinity gradient; phosphorus; speciation; migration and transformation

磷是生物体遗传代谢、能量传输和细胞膜合成等过程所必需的生源要素, 在调节水体初级生产力方面具有关键作用^[1-3]. 过量的磷进入水体会引发水体富营养化进而导致水华或赤潮等现象^[4], 然而水体的磷浓度过低亦可能致使鱼类减产或破坏浮游生物的群落结构^[5-7]. 维持适宜的磷浓度对于水生生态系统的健康和稳定性具有重要意义. 然而, 珠江三角洲快速的城镇化进程与人口膨胀增加了珠江河口的水环境负担^[8], 导致赤潮频发^[9, 10], 而磷是藻类生长的主要限制元素^[11, 12].

河流输送的磷是河口主要的磷来源方式, 其中铁(Fe)在磷迁移过程中起到“传输带”作用: 无机磷被悬浮颗粒物上的Fe吸附或结合, 运移至河口并沉降于沉积物中, 在缺氧条件下的Fe氧化物还原溶解过

程中被释放^[13, 14]. 高强度 SO_4^{2-} 还原环境产生的二价硫化物($\sum \text{S}^{2-}$)可以与Fe反应, 形成非溶解性 FeS_2 并降低其对无机磷的吸附能力^[15-17]. 由于环境中Fe的含量往往远高于锰(Mn), 以往的研究更多关注Fe循环对水环境中磷循环的影响^[18-24]; 然而, Mn氧化物具有低Zeta电位、高比表面积和高表面电荷数, 对水体中无机磷迁移转化行为的影响不容忽视^[25-27]. 此外, 铝(Al)的氢氧化物对磷也有良好的吸附亲和力^[28, 29]. 华

收稿日期: 2023-01-03; 修订日期: 2023-03-10

基金项目: 国家自然科学基金项目(42077376, 41961144027); 中国科学院青年创新促进会项目(2022352); 中国科学院退化生态系统植被恢复与管理重点实验室开放基金项目(VRMDE2202)

作者简介: 李睿(1995~), 男, 博士研究生, 主要研究方向为河口水环境过程, E-mail: lirui37@mail2.sysu.edu.cn

* 通信作者, E-mail: nvtoo@sina.com; chenjiyao@mail.sysu.edu.cn

南地区富含 Fe、Mn 和 Al 的土壤在降水冲刷作用下进入水环境可以影响磷的迁移转化行为^[30,31]. 珠三角城市河流中发现了磷和 Mn 之间紧密的地球化学循环过程^[15], 然而珠江河口却主要是铁-磷耦合的迁移机制^[13,32]. 这种差异可能源于磷在河流输送的过程中发生的形态转化. 关于河口水体磷形态的研究已多有报道^[33-36], 但是鲜有研究区分 Fe、Mn 和 Al 在磷迁移过程中的作用. 由于海水中 Mn 氧化物对无机磷的吸附亲和力低于 Fe 氧化物和 Al 氢氧化物^[29,37], 本文提出咸-淡水交互区常量金属 Mn 对无机磷的输送过程起到关键“载-卸”作用的科学假设: Mn 氧化物吸附富集淡水环境的无机磷在高盐度水体中释放. 基于此, 本文以珠江河口咸-淡水交互区为研究区, 探索地表水磷及其形态的时空变化规律, 揭示沿盐度梯度常量金属 (Fe、Mn 和 Al) 对磷迁移转化的影响, 研究结果可以提升河口地区磷循环的认知, 以期对珠江河口削减磷负荷提供科学依据.

1 材料与方法

1.1 研究区概况与样品采集

珠江流域 (112° 14' ~ 115° 53' E, 21° 31' ~ 26° 49' N) 由西江、北江、东江和珠江三角洲诸河组成, 流域面积 453 690 km², 多年平均年径流量 3.38 × 10¹¹ m³. 属于热带和热带季风气候, 降水主要集中在 4 ~ 10 月. 各水系交汇于珠江三角洲平原, 形成放射状水网入海, 其中东部 4 个入海口虎门、蕉门、洪奇沥和横门的水流汇入伶仃洋, 潮汐属于不正规半日潮 (图 1).



图 1 珠江河口表层水采样点示意

Fig. 1 Sampling sites for the surface water in the Pearl River Estuary

1.2 样品采集与现场测定

如图 1 所示, 沿盐度梯度在珠江口干流与伶仃洋水域设置 5 个采样点位: ①中山大学码头 (ZD) 位于珠江前航道; ②海鸥岛 (HOD) 是冲积而成的内河岛屿, 岛上以种养业为主; ③舢板洲 (SBZ) 位于广州南沙港附近; ④淇澳岛 (QAD) 北部是红树林保护区; ⑤桂山岛 (GSD) 主要发展旅游业, 也是重要的网箱养殖基地. 本研究于 2021 年 4 月初旱季与 7 月中旬雨季, 在高潮、低潮以及高低潮或低高潮时段采集地表水样品 (在不同潮位时段采集以增加样品的代表性), 用 0.45 μm 孔径醋酸纤维滤膜 (提前烘干、称重) 分离溶解态物质和悬浮颗粒物 (SPM). 采用便携式多功能分析仪 (HQ-40d; Hach, Loveland, USA) 现场测定 pH、盐度、温度和溶解氧 (DO). 采用酸碱滴定试剂盒 (Mquant Alkalinity Test; Merk, USA) 现场测定重碳酸根 (HCO₃⁻).

1.3 实验分析方法

地表水溶解阴离子 Cl⁻ 和 SO₄²⁻ 浓度用离子色谱仪 (ICS-900; Dionex, USA) 测定. Na⁺、K⁺、Ca²⁺、Mg²⁺ 等溶解阳离子浓度用电感耦合等离子体原子发射光谱仪 (ICP-AES; IRIS, USA) 测定. 溶解态无机磷 (dissolved inorganic phosphorus, DIP) 使用磷钼蓝法测定^[38], 溶解态总磷 (dissolved total phosphorus, DTP) 经过硫酸钾消解后用磷钼蓝法测定, 溶解态有机磷 (dissolved organic phosphorus, DOP) 为 DTP 和 DIP 之差.

醋酸纤维滤膜上的悬浮颗粒物样品在 60°C 下烘干至恒重后计算其质量. 用陶瓷刀将滤膜对半分, 一半滤膜用 1 mol·L⁻¹ 盐酸浸提 24 h 测定颗粒态无机磷 (particulate inorganic phosphorus, PIP), 另一半滤膜用 H₂SO₄-HClO₄ 消解后测定颗粒态总磷 (particulate total phosphorus, PTP)、颗粒态铝 (particulate aluminum, PAI)、颗粒态铁 (particulate iron, PFe) 和颗粒态锰 (particulate manganese, PMn) 等. 上述浸提液与消解液以 2,4-二硝基苯酚为指示剂用 4 mol·L⁻¹ NaOH 调节至 pH≈3 后, 用磷钼蓝法测定其中磷含量. 颗粒态有机磷 (particulate organic phosphorus, POP) 为 PTP 和 PIP 之差, 总磷 (total phosphorus, TP) 则为 DTP 和 PTP 之和.

1.4 数据分析方法

本研究涉及的阴阳离子数据经过离子电荷平衡计算验证. 地表水总溶解性固体 (total dissolved solid, TDS) 为所有溶解阴阳离子质量浓度总和. 采用 IBM SPSS Statistics 22 进行数据统计分析, 如果参数符合正态分布, 选用 Pearson 相关及线性相关分析参数间的相关关系; 否则, 采用非参数 Spearman 进行相关分析. 采用非参数用 Origin 2021 描绘 Piper 三线图和

Gibbs 图, 拟合水质理化参数间的二元回归方程。

2 结果与讨论

2.1 地表水基本理化性质

如表 1 所示, 研究区地表水 pH 范围为 7.19 ~ 8.03, 平均值为 7.59, 呈弱碱性。盐度范围为 0.14‰ ~ 21.12‰, 属于淡水 (< 0.5‰) 或微咸水 (0.5‰ ~ 30‰), 其中 HOD 点位在旱季和雨季分别属于微咸水

与淡水; 此外, SBZ、QAD 和 GSD 点位在雨季时受地表径流的稀释作用较为明显。ρ(DO) 范围为 4.25 ~ 8.60 mg·L⁻¹, 旱季时的水体 DO 浓度总体上高于雨季; 其中, ZD 点位的水体 DO 浓度显著低于其他点位 (P < 0.05), 可能与城市排放的污染物在分解过程中消耗了大量溶解氧有关。ρ(SPM) 范围为 5.27 ~ 79.23 μg·L⁻¹, 雨季时受降水冲刷作用影响高于旱季。

表 1 珠江河口地表水基本理化性质¹⁾

Table 1 Physiochemical properties of the surface water in the Pearl River Estuary

季节	采样点	pH	温度/°C	盐度/‰	ρ(DO)/mg·L ⁻¹	ρ(SPM)/mg·L ⁻¹
旱季	ZD	8.03 ± 0.10a	24.18 ± 0.98a	0.18 ± 0.00e	4.25 ± 0.78b	9.59 ± 4.60ab
	HOD	7.47 ± 0.09b	23.88 ± 1.15a	3.35 ± 0.39d	7.59 ± 0.67a	56.11 ± 43.01a
	SBZ	7.60 ± 0.15b	25.03 ± 0.67a	8.37 ± 0.91c	8.18 ± 0.14a	10.83 ± 12.68ab
	QAD	7.59 ± 0.64b	25.00 ± 0.63a	11.52 ± 0.20b	8.60 ± 0.53a	18.93 ± 11.16ab
	GSD	7.52 ± 0.08b	23.10 ± 0.66a	21.12 ± 0.03a	8.51 ± 0.22a	5.27 ± 1.90b
雨季	ZD	7.51 ± 0.15ab	31.00 ± 1.55a	0.14 ± 0.01e	4.68 ± 1.15e	22.88 ± 2.24ab
	HOD	7.52 ± 0.21ab	32.27 ± 1.94a	0.23 ± 0.00b	5.82 ± 0.19b	79.23 ± 48.60a
	SBZ	7.19 ± 0.11b	30.30 ± 2.07a	3.64 ± 1.21ab	6.62 ± 0.50ab	26.31 ± 8.01ab
	QAD	7.37 ± 0.19ab	29.80 ± 2.05a	4.92 ± 1.61ab	6.37 ± 0.12ab	28.47 ± 19.01ab
	GSD	7.93 ± 0.12a	29.27 ± 1.12a	17.96 ± 1.11a	7.35 ± 0.34a	11.50 ± 6.34b

1) 不同小写字母表示不同点位存在显著性差异 (P < 0.05)

2.2 水化学特征

如图 2 所示, 研究区地表水 ρ(TDS) 范围为 270 ~ 37 500 mg·L⁻¹. GSD、QAD、SBZ 和 HOD (旱季) 点位的 ρ(Cl⁻)/ρ(Cl⁻+HCO₃⁻) 和 ρ(Na⁺)/ρ(Na⁺+Ca²⁺) 均接近 1, 说明这些点位的地表水主要受蒸发浓缩作用控制, 受海水的影响; 而 ZD 和 HOD (雨季) 点位为陆地流域水岩作用控制, 可被视为淡水水体^[39]. HOD 点位在雨季和旱季时分属不同水化学类型, 说明该

点位于咸-淡水交互作用的界面附近, 理化性质取决于径流与潮汐作用的相对强度. 该点位的水流方向可能随潮汐涨落出现相反的变化, 而这种复杂多变的水动力条件不利于悬浮颗粒物的沉降, 导致地表水中高浓度的悬浮颗粒物 (表 1). 综合基本理化性质及水化学特征将采样点划分为 3 类: 淡水区 (ZD)、咸-淡水界面 (HOD)、微咸水区 (SBZ、QAD、GSD).

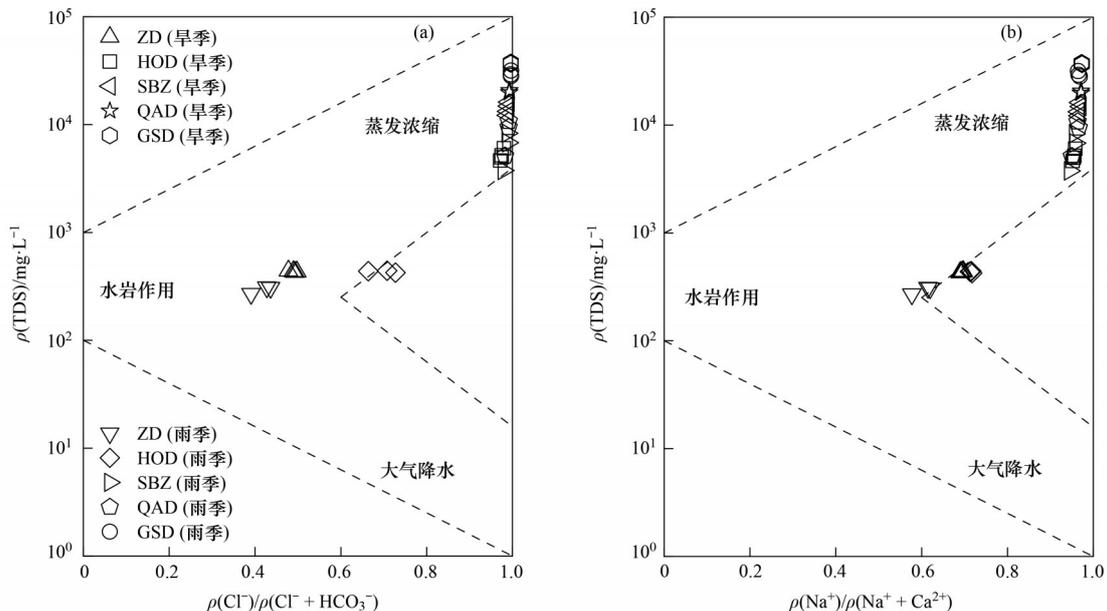


图 2 珠江河口地表水 Gibbs 图

Fig. 2 Gibbs map of the surface water in the Pearl River Estuary

2.3 珠江河口地表水磷的时空分布特征

珠江河口地表水 $\rho(\text{TP})$ 范围为28.88~233.68 $\mu\text{g}\cdot\text{L}^{-1}$,从淡水区向微咸水区呈现降低趋势(表2). 随水流迁移距离的增加,咸水逐渐稀释了磷浓度;此外,河口区域的水流趋缓,有利于颗粒态磷的沉降作用. 旱季时,地表水 $\rho(\text{TP})$ (均值:95.93 $\mu\text{g}\cdot\text{L}^{-1}$)略低于雨季(均值:116.18 $\mu\text{g}\cdot\text{L}^{-1}$). 一方面,雨季的降水增强了磷的面源负荷,可能是总磷浓度升高的主要原因;另一方面,径流量增大使咸-淡水界面向河口区推移,扩大了陆源物质输送的影响范围. 如表2所示,水体中主要的磷形态为DIP(10.98~54.41 $\mu\text{g}\cdot\text{L}^{-1}$),占TP的37.3%,从淡水区到微咸水区呈现显著下降的趋势($P < 0.05$);旱季时,ZD和HOD点位的DIP浓

度高于雨季,而微咸水区点位却低于雨季,这主要是因为旱季采样期间正值浮游植物生长期,大量无机磷被吸收利用^[11, 33]. $\rho(\text{DOP})$ 范围为9.04~50.80 $\mu\text{g}\cdot\text{L}^{-1}$,占TP的21.0%;雨季时,DOP从淡水区到咸水区呈现显著的降低趋势($P < 0.05$),而旱季无显著空间差异($P > 0.05$). 水体中的DOP可能与降水导致的面源污染有关,雨季时加剧了这一过程. $\rho(\text{PIP})$ 和 $\rho(\text{POP})$ 范围分别为2.54~74.67 $\mu\text{g}\cdot\text{L}^{-1}$ 和4.39~61.24 $\mu\text{g}\cdot\text{L}^{-1}$,分别占TP的22.7%和19.0%,雨季时PIP和POP普遍大于旱季,随盐度的升高大致呈现降低的趋势. 而雨季时,GSD点位的PIP和POP浓度较QAD点位更高,说明该点位可能存在除径流输入以外的颗粒态磷来源.

表2 珠江河口地表水总磷及磷形态浓度¹⁾/ $\mu\text{g}\cdot\text{L}^{-1}$

Table 2 Concentrations of TP and phosphorus speciation in the surface water in the Pearl River Estuary/ $\mu\text{g}\cdot\text{L}^{-1}$

季节	磷形态	ZD	HOD	SBZ	QAD	GSD
旱季	TP	156.56 ± 23.53a	139.70 ± 50.84a	60.99 ± 12.39b	70.39 ± 11.15b	28.88 ± 4.16c
	DIP	54.41 ± 5.22a	50.64 ± 3.32a	28.12 ± 3.65b	24.20 ± 3.77b	10.98 ± 3.85c
	DOP	18.90 ± 9.13a	16.08 ± 3.84a	14.92 ± 3.41a	19.22 ± 4.07a	10.97 ± 2.68a
	PIP	49.97 ± 15.15a	44.45 ± 29.78a	9.02 ± 6.86b	13.02 ± 2.48b	2.54 ± 0.67c
	POP	33.28 ± 6.14a	28.53 ± 15.01ab	8.92 ± 4.82ab	13.95 ± 1.63b	4.39 ± 0.81c
雨季	TP	233.68 ± 45.60a	133.72 ± 31.16b	79.07 ± 19.08b	73.08 ± 20.49b	61.33 ± 14.02b
	DIP	46.97 ± 15.47a	33.13 ± 2.80ab	40.71 ± 2.53ab	35.15 ± 4.27ab	16.29 ± 5.63c
	DOP	50.80 ± 13.42a	36.89 ± 2.87b	17.54 ± 11.11bc	9.04 ± 1.06bc	9.25 ± 5.73c
	PIP	74.67 ± 17.96a	32.70 ± 20.26ab	12.09 ± 2.42ab	14.97 ± 8.73ab	20.99 ± 6.70c
	POP	61.24 ± 13.76a	30.99 ± 11.23b	8.72 ± 5.70b	13.91 ± 8.31b	14.79 ± 5.30b

1)不同小写字母表示不同点位存在显著性差异($P < 0.05$)

珠江口水体磷主要以溶解态(41.9%~75.5%)的形式进行迁移,不同点位的DTP和PTP的占比有明显差异,表明各形态的磷在不同水动力、水环境条件下的迁移转化过程迥异(图3). 从淡水区点位ZD到微咸水区点位SBZ,水动力条件减弱,促进了PTP沉降,导致其比例降低;而在微咸水区(除雨季GSD点),DTP的比例随盐度没有明显的变化. GSD点位雨季的PTP比例显著大于旱季($P < 0.05$),与SPM浓度的季节变化特征一致(表1). 这可能与桂山岛的人类活动污染排放有关,而降水事件则进一步加剧了GSD局部的陆源磷负荷.

由于各采样点受到的海水稀释作用差异,磷与盐度的关系曲线可以更准确地反映其在咸-淡水交互区的迁移行为(图4). 如图4(a)所示,TP浓度沿盐度梯度呈现负对数下降趋势,在盐度小于5‰的区域大幅减少,说明TP除受到咸水的稀释作用外还发生了明显的沉降过程. 在径流、潮汐和咸淡水混合等因素的作用下,可能出现滞流或往复流现象,使悬浮颗粒物在原位大量沉降,并在口门区附近形成拦门

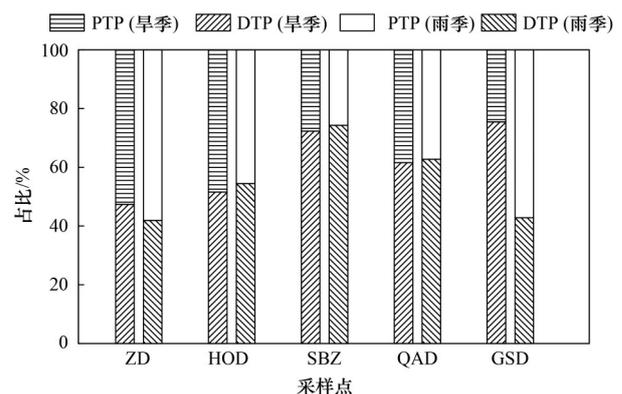


图3 珠江口水体不同磷形态(溶解态总磷和颗粒态总磷)的占比
Fig. 3 Proportion of phosphorus speciation (DTP & PTP) in the surface water in the Pearl River Estuary

沙^[40]. 例如海鸥沙,就是近代珠江三角洲河网区快速沉积形成沙坝,而后进一步发育扩大^[41]. TP浓度沿盐度梯度分布的季节差异不明显. 地表水中不同形态的无机磷均随盐度升高而下降(图4);溶解态磷(DIP和DOP)主要受到咸水和淡水混合后的稀释作用,而颗粒态磷(PIP和POP)受到稀释作用的同时在沿程上

发生沉降.

2.4 常量金属元素对无机磷迁移过程的影响

如表 3 所示, 旱季时, 磷及其各形态均与 PFe、PMn 和 PAI 呈显著正相关 ($P < 0.05$); 而雨季时, 仅发现 TP、PIP 和 POP 与 PMn 之间的显著正相关关系 ($P < 0.05$). 这说明磷的迁移、沉降过程与 PFe、PMn 和 PAI 密切相关. 由于悬浮颗粒物主要来源于面源负荷, 因此受雨季降水增强的影响, 出现磷与常量金属相关关系的部分解耦^[42]. 此外, PMn 与磷及其形态之间的相关系数较 PFe 和 PAI 更高 (表 3), 表明 PMn 在磷的迁移过程中可能发挥了更重要的作用.

表 3 不同季节磷(形态)与颗粒态铁、颗粒态锰和颗粒态铝相关性分析¹⁾

Table 3 Correlation analysis between phosphorus (including speciation), PFe, PMn, and PAI in different seasons

季节	磷(形态)	PFe	PMn	PAI
旱季	TP	0.721**	0.889**	0.736**
	DIP	0.475*	0.669**	0.504*
	DOP	0.548*	0.598**	0.542*
	PIP	0.738**	0.905**	0.754**
	POP	0.730**	0.907**	0.738**
雨季	TP	0.046	0.618*	0.032
	DIP	0.118	0.232	0.136
	DOP	-0.350	0.268	-0.371
	PIP	0.214	0.839**	0.186
	POP	0.089	0.754**	0.061

1)*和**分别表示在 0.05 和 0.01 水平上的显著相关

如图 5 所示, PIP 与 PFe、PMn 和 PAI 之间在淡水区、咸-淡水界面和微咸水区都存在显著正线性相关关系 ($P < 0.05$), 说明悬浮颗粒物上的 Fe、Mn 和 Al 与无机磷在咸-淡水交互区的吸附-解吸过程有关, 证实了 Fe、Mn 和 Al 携带磷的理论假设. 不同水域

PFe、PMn 和 PAI 与 PIP 拟合曲线斜率均呈现相同大小顺序: 淡水区 > 咸-淡水交互区 > 微咸水区 (图 5). 这表示在盐度越高的水域, 等量的 PFe、PMn 和 PAI 携带的无机磷越少, 主要原因为高浓度阴离子的竞争吸附作用促进了吸附态无机磷的解吸. 而且从淡水区到咸-淡水交互区的拟合曲线斜率变幅 (2.4 ~ 5.7 倍) 远大于从咸-淡水交互区到微咸水区 (1.3 ~ 1.6 倍), 说明 PIP 的解吸过程主要发生在颗粒物通过咸-淡水界面的过程. 当悬浮颗粒物通过咸-淡水界面进入盐度更高的水域时, 无机磷的释放量相对较少, 可能是因为此时 PIP 主要以更稳定的 Fe、Mn 或 Al 结合态的形式存在.

固-液分配系数表征地表水中 PIP 与 DIP 之间的配分关系, 可以反映悬浮颗粒物上无机磷的吸附-解吸特征:

$$K_d = \frac{\rho(\text{PIP})}{\rho(\text{DIP}) \times \rho(\text{SPM})}$$

式中, K_d 为无机磷的固-液分配系数 ($\text{L} \cdot \text{mg}^{-1}$), $\rho(\text{PIP})$ 为珠江口地表水 PIP 的质量浓度 ($\mu\text{g} \cdot \text{L}^{-1}$); $\rho(\text{DIP})$ 为珠江口地表水 DIP 的质量浓度 ($\mu\text{g} \cdot \text{L}^{-1}$); $\rho(\text{SPM})$ 是珠江口地表水 SPM 的质量浓度 ($\text{mg} \cdot \text{L}^{-1}$). 如图 6 所示, 旱季时淡水点位 ZD 的 K_d ($0.101 \text{ L} \cdot \text{mg}^{-1}$) 高于雨季 (均值: $0.074 \text{ L} \cdot \text{mg}^{-1}$). 悬浮颗粒物能起到“缓冲”作用: 当水体 DIP 被降水稀释时, 悬浮颗粒物能够释放 PIP, 维持固-液相间 DIP 的动态平衡^[43, 44]. 咸-淡水界面点位 HOD 的 K_d ($0.007 \sim 0.030 \text{ L} \cdot \text{mg}^{-1}$) 均低于 ZD ($0.053 \sim 0.130 \text{ L} \cdot \text{mg}^{-1}$), 也证实了 PIP 在通过咸-淡水界面时被大量释放. 在微咸水水域 (盐度 $> 0.5\text{‰}$), K_d 与盐度存在显著正相关关系 ($P < 0.001$), 而 DIP 随盐度的升高而减小 (图 4), 说明微咸水区内 PIP 的稳

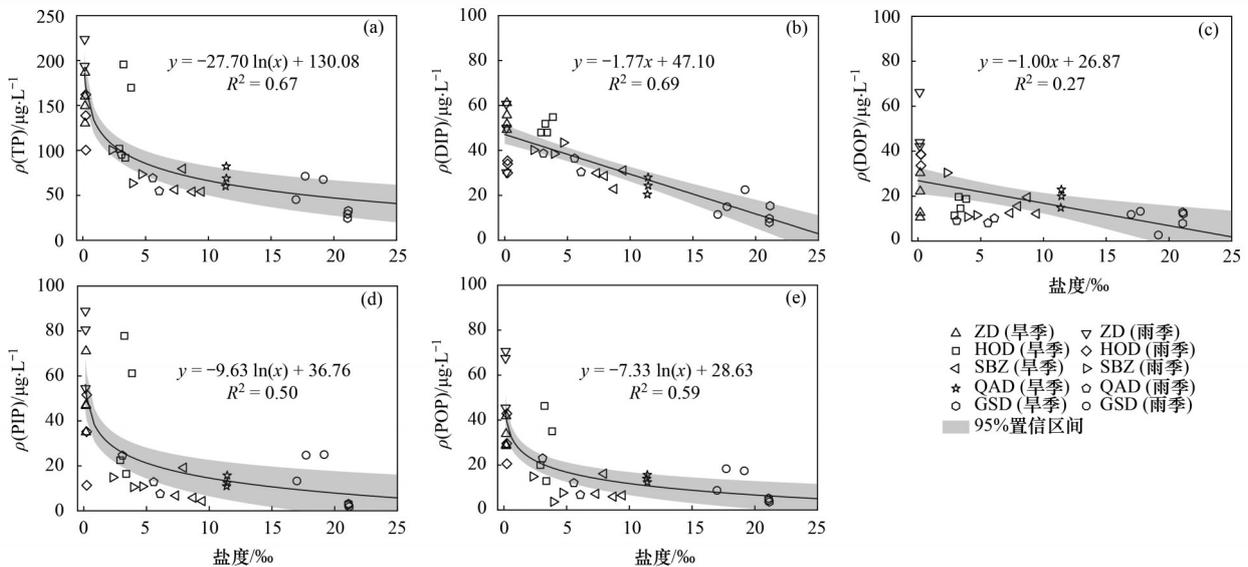


图 4 珠江口地表水磷及其形态与盐度的关系

Fig. 4 Relationship between P and salinity of the surface water in the Pearl River Estuary

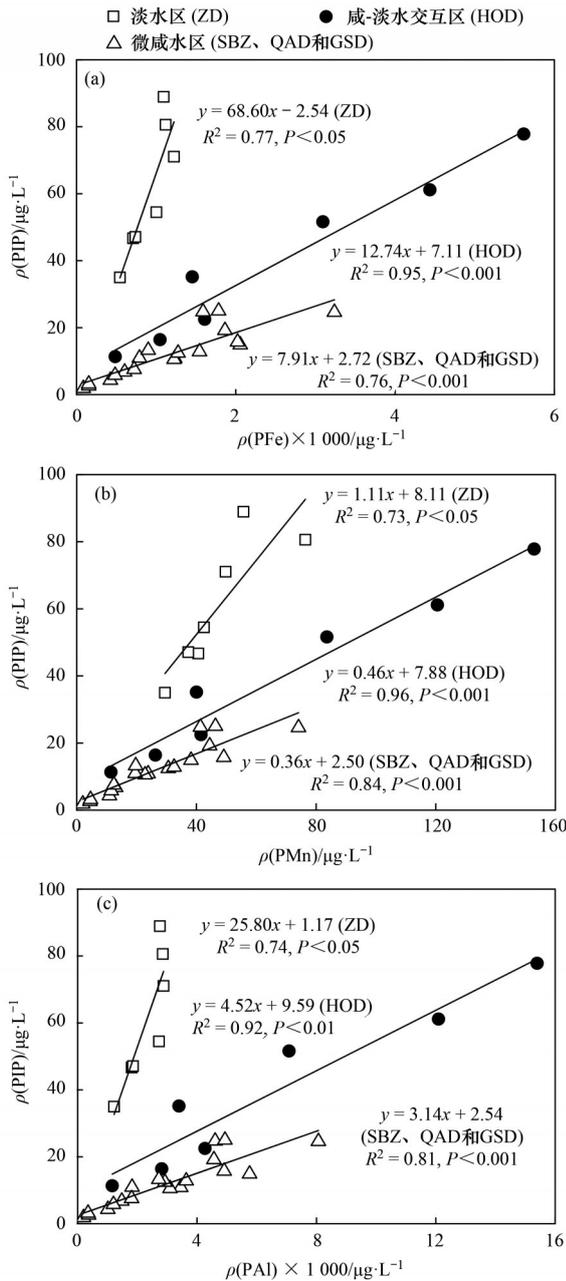


图5 珠江口地表水颗粒态无机磷与颗粒态铁、锰和铝的关系
Fig. 5 Relationships between PIP, PFe, PMn, and PAI in the surface water in the Pearl River Estuary

定性随盐度而升高,以更稳定的Fe、Mn或Al结合态存在。

Fe、Mn和Al氧化物或氢氧化物能通过物理吸附、络合反映或化学结合的形式与磷一起迁移,然而珠江河口PFe、PMn和PAI对PIP吸附-释放特征的影响程度迥异。如图7所示,ZD点到QAD点的PMn与 K_d 相关关系($R=0.93, P < 0.001$)较PFe($R=0.53, P < 0.01$)和PAI($R=0.46, P < 0.05$)更显著,说明无机磷的吸附-释放过程与Mn有更紧密的联系。天然Mn氧化物通过静电吸附或络合反应的机制吸附无机磷,但是这种反应是完全可逆的^[18, 26, 45]。尤其在咸水环境

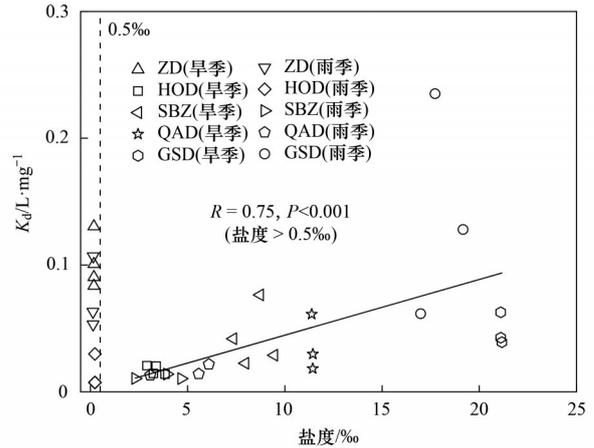


图6 珠江口地表水无机磷的固-液分配系数(K_d)与盐度的关系
Fig. 6 Relationship between solid-liquid phase partitioning coefficient (K_d) of inorganic phosphorus and salinity in the surface water in the Pearl River Estuary

中,钙和镁离子可以增强阴离子和锰氧化物表面之间的相互作用,一定程度上降低锰氧化物对无机磷的吸附^[37]。相对而言,Fe氧化物表面的吸附点位在 $\text{pH} > 7$ 的海水中对无机磷的吸附亲和力都高于Mn氧化物,而且Al的氢氧化物对无机磷的吸附选择性远高于 Cl^- 和 SO_4^{2-} 等其他阴离子,因此Fe和Al携带的PIP在高盐度环境中解吸释放的可能性更小。那么,通过咸-淡水界面后,PIP沿盐度升高梯度的释放主要来源于Mn氧化物,证实了Mn在无机磷迁移过程中起到了关键的“卸-载”作用。PIP与PFe和PAI之间的显著正相关关系($P < 0.05$)说明Fe和Al是无机磷的良好载体(图5),但是在咸水环境依然保持相对稳定,不具备“卸”磷的作用。华南地区富锰的土壤条件放大了水环境Mn氧化物对磷迁移的影响,相似的情况也在福建九龙江河口发现^[30, 31]。在GSD点, K_d 仅与PMn具有显著相关关系($P < 0.01$),且拟合曲线偏离其他点位(图7),这说明PIP除了珠江主流输送,也有一部分来源于桂山岛等周围岛屿。桂山岛与珠三角污染源性质的差异可能是该点位 K_d 与PFe和PAI解耦的主要原因。

3 结论

河口区的磷主要来源于陆地径流带来的面源负荷,总磷的质量浓度沿着盐度梯度呈下降趋势,各形态占比大小顺序依次为: $\text{DIP} > \text{DOP} > \text{PIP} > \text{POP}$ 。悬浮颗粒物中的Fe、Mn和Al的氧化物或氢氧化物吸附并携带无机磷向河口迁移。微咸水环境中PMn是无机磷吸附-解吸的关键控制因素,受阴离子竞争吸附作用而解吸。这证明了Mn氧化物在咸-淡水交互区无机磷迁移过程中起着重要的“载-卸”作用:将淡水环境中吸附的无机磷携带至高盐度水域释放。咸水

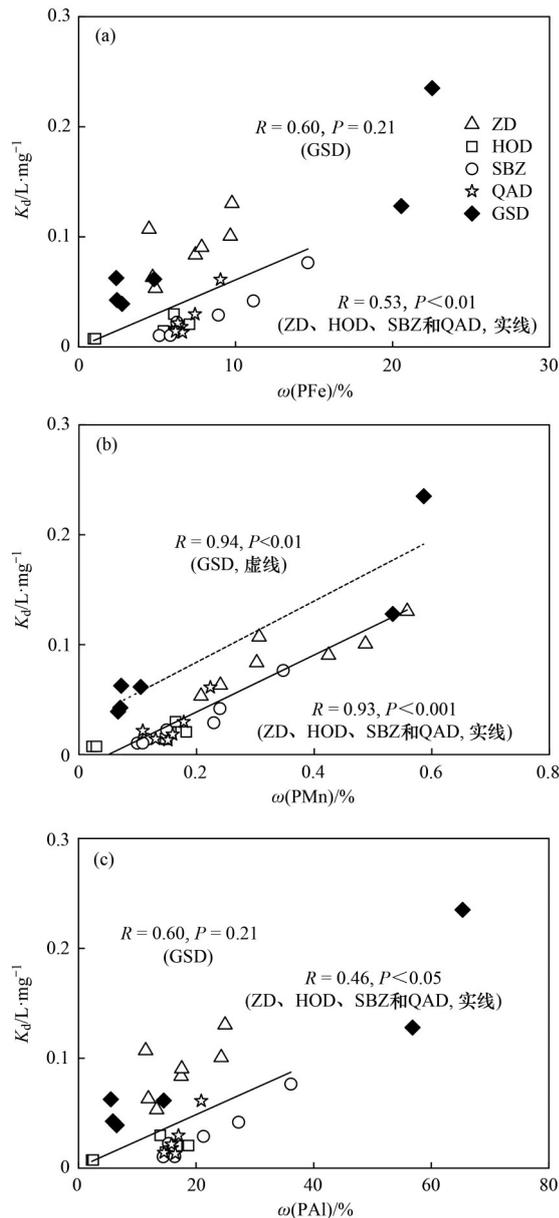


图7 珠江口地表水无机磷的固-液分配系数与颗粒态的Fe、Mn和Al质量分数相关性

Fig. 7 Relationships between solid-liquid phase partitioning coefficient (K_d) of inorganic phosphorus and the mass percentage concentrations of PFe, PMn, and PAI in the surface water in the Pearl River Estuary

区内, PIP的稳定性沿盐度梯度增大, 转为更稳定的Fe、Mn或Al结合态磷。上述结论验证了本文的理论假设, 并强调了氧化环境中Mn氧化物对于无机磷环境行为的重要意义。

参考文献:

- [1] Némery J, Garnier J. The fate of phosphorus [J]. *Nature Geoscience*, 2016, **9**(5): 343-344.
- [2] Conley D J, Paerl H W, Howarth R W, *et al.* Controlling eutrophication: nitrogen and phosphorus [J]. *Science*, 2009, **323** (5917): 1014-1015.
- [3] Canfield D E, Bjerrum C J, Zhang S C, *et al.* The modern phosphorus cycle informs interpretations of Mesoproterozoic Era

phosphorus dynamics [J]. *Earth-Science Reviews*, 2020, **208**, doi: 10.1016/j.earscirev.2020.103267.

- [4] Sellner K G, Doucette G J, Kirkpatrick G J. Harmful algal blooms: causes, impacts and detection [J]. *Journal of Industrial Microbiology and Biotechnology*, 2003, **30**(7): 383-406.
- [5] Soomets T, Kutser T, Wüest A, *et al.* Spatial and temporal changes of primary production in a deep peri-alpine lake [J]. *Inland Waters*, 2019, **9**(1): 49-60.
- [6] Yamamoto T. The Seto Inland Sea—eutrophic or oligotrophic? [J]. *Marine Pollution Bulletin*, 2003, **47**(1-6): 37-42.
- [7] Irizuki T, Hirose K, Ueda Y, *et al.* Ecological shifts due to anthropogenic activities in the coastal seas of the Seto Inland Sea, Japan, since the 20th century [J]. *Marine Pollution Bulletin*, 2018, **127**: 637-653.
- [8] Gao L, Wang Z W, Shan J J, *et al.* Aquatic environmental changes and anthropogenic activities reflected by the sedimentary records of the Shima River, Southern China [J]. *Environmental Pollution*, 2017, **224**: 70-81.
- [9] Huang X P, Huang L M, Yue W Z. The characteristics of nutrients and eutrophication in the Pearl River estuary, South China [J]. *Marine Pollution Bulletin*, 2003, **47**(1-6): 30-36.
- [10] Ip C C M, Li X D, Zhang G, *et al.* Over one hundred years of trace metal fluxes in the sediments of the Pearl River Estuary, South China [J]. *Environmental Pollution*, 2004, **132**(1): 157-172.
- [11] 韦桂秋, 王华, 蔡伟叙, 等. 近10年珠江口海域赤潮发生特征及原因初探 [J]. *海洋通报*, 2012, **31**(4): 466-474.
- Wei G Q, Wang H, Cai W X, *et al.* 10-year retrospective analysis on the harmful algal blooms in the Pearl River Estuary [J]. *Marine Science Bulletin*, 2012, **31**(4): 466-474.
- [12] Yin K D, Qian P Y, Chen J C, *et al.* Dynamics of nutrients and phytoplankton biomass in the Pearl River estuary and adjacent waters of Hong Kong during summer: preliminary evidence for phosphorus and silicon limitation [J]. *Marine Ecology Progress Series*, 2000, **194**: 295-305.
- [13] Gao L, Li R, Liang Z B, *et al.* Remobilization mechanism and release characteristics of phosphorus in saline sediments from the Pearl River Estuary (PRE), South China, based on high-resolution measurements [J]. *Science of the Total Environment*, 2020, **703**, doi: 10.1016/j.scitotenv.2019.134411.
- [14] Jordan T E, Cornwell J C, Boynton W R, *et al.* Changes in phosphorus biogeochemistry along an estuarine salinity gradient: the iron conveyor belt [J]. *Limnology and Oceanography*, 2008, **53** (1): 172-184.
- [15] Li R, Gao L, Wu Q R, *et al.* Release characteristics and mechanisms of sediment phosphorus in contaminated and uncontaminated rivers: a case study in South China [J]. *Environmental Pollution*, 2021, **268**, doi: 10.1016/j.envpol.2020.115749.
- [16] Pan F, Guo Z R, Cai Y, *et al.* Kinetic exchange of remobilized phosphorus related to phosphorus-iron-sulfur biogeochemical coupling in coastal sediment [J]. *Water Resources Research*, 2019, **55**(12): 10494-10517.
- [17] Xiong Y J, Guilbaud R, Peacock C L, *et al.* Phosphorus cycling in Lake Cadagno, Switzerland: a low sulfate euxinic ocean analogue [J]. *Geochimica et Cosmochimica Acta*, 2019, **251**: 116-135.
- [18] Yan Y P, Wan B, Mansor M, *et al.* Co-sorption of metal ions and inorganic anions/organic ligands on environmental minerals: a review [J]. *Science of the Total Environment*, 2022, **803**, doi: 10.1016/j.scitotenv.2021.149918.
- [19] Chen Q, Chen J G, Wang J F, *et al.* *In situ*, high-resolution

- evidence of phosphorus release from sediments controlled by the reductive dissolution of iron-bound phosphorus in a deep reservoir, southwestern China[J]. *Science of the Total Environment*, 2019, **666**: 39-45.
- [20] Gao Y L, Liang T, Tian S H, *et al.* High-resolution imaging of labile phosphorus and its relationship with iron redox state in lake sediments[J]. *Environmental Pollution*, 2016, **219**: 466-474.
- [21] Ding S M, Han C, Wang Y P, *et al.* In situ, high-resolution imaging of labile phosphorus in sediments of a large eutrophic lake[J]. *Water Research*, 2015, **74**: 100-109.
- [22] Hu M J, Sardans J, Le Y X, *et al.* Phosphorus mobilization and availability across the freshwater to oligohaline water transition in subtropical estuarine marshes[J]. *CATENA*, 2021, **201**, doi: 10.1016/j.catena.2021.105195.
- [23] 张雪, 朱波. 三峡库区支流库湾消落带土壤磷形态赋存特征及其释放风险[J]. *环境科学*, 2023, **44**(5):2574-2582.
Zhang X, Zhu B. Distribution and release potential of soil phosphorus fractions in water-level-fluctuation zone of the Tributary Bay, Three Gorges Reservoir[J]. *Environmental Science*, 2023, **44**(5):2574-2582.
- [24] 刘笑天, 刘军, 王以斌, 等. 不同溶解氧条件下沉积物-水体体系磷循环[J]. *环境科学*, 2022, **43**(12): 5571-5584.
Liu X T, Liu J, Wang Y B, *et al.* Phosphorus cycling in a sediment-water system controlled by different dissolved oxygen levels of overlying water[J]. *Environmental Science*, 2022, **43**(12): 5571-5584.
- [25] Zaman M I, Mustafa S, Khan S, *et al.* The effects of phosphate adsorption on the surface characteristics of Mn oxides [J]. *Separation Science and Technology*, 2013, **48**(11): 1709-1716.
- [26] Ouvrad S, Simonnot M O, Sardin M. Reactive behavior of natural manganese oxides toward the adsorption of phosphate and arsenate [J]. *Industrial & Engineering Chemistry Research*, 2002, **41**(11): 2785-2791.
- [27] 蔡言安, 毕学军, 张嘉凝, 等. 铁锰原位氧化产物吸附微量磷的实验[J]. *环境科学*, 2018, **39**(7): 3222-3229.
Cai Y A, Bi X J, Zhang J N, *et al.* Trace amounts of phosphorus removal based on the in-suit oxidation products of iron or manganese in a biofilter [J]. *Environmental Science*, 2018, **39**(7): 3222-3229.
- [28] Jensen H S, Reitzel K, Egemose S. Evaluation of aluminum treatment efficiency on water quality and internal phosphorus cycling in six Danish lakes [J]. *Hydrobiologia*, 2015, **751**(1): 189-199.
- [29] Tanada S, Kabayama M, Kawasaki N, *et al.* Removal of phosphate by aluminum oxide hydroxide[J]. *Journal of Colloid and Interface Science*, 2003, **257**(1): 135-140.
- [30] 黄丽, 洪军, 谭文峰, 等. 我国几种亚热带土壤铁锰胶膜的微形貌和元素分布特征[J]. *自然科学进展*, 2006, **16**(9): 1122-1129.
- [31] Pan F, Liu H T, Guo Z R, *et al.* Metal/metalloid and phosphorus characteristics in porewater associated with manganese geochemistry: a case study in the Jiulong River Estuary, China [J]. *Environmental Pollution*, 2019, **255**, doi: 10.1016/j.envpol.2019.113134.
- [32] 翁焕新, 孙向卫, 陈静峰, 等. 珠江口沉积铁-磷的富集对赤潮频发的潜在作用[J]. *中国科学 D 辑: 地球科学*, 2006, **36**(12): 1122-1130.
- [33] Li R H, Xu J, Li X F, *et al.* Spatiotemporal variability in phosphorus species in the Pearl River Estuary: influence of the river discharge [J]. *Scientific Reports*, 2017, **7**(1), doi: 10.1038/s41598-017-13924-w.
- [34] Ke S, Zhang P, Ou S J, *et al.* Spatiotemporal nutrient patterns, composition, and implications for eutrophication mitigation in the Pearl River Estuary, China [J]. *Estuarine, Coastal and Shelf Science*, 2022, **266**, doi: 10.1016/j.ecss.2022.107749.
- [35] Zhang M Z, Krom M D, Lin J J, *et al.* Effects of a storm on the transformation and export of phosphorus through a subtropical river-turbid estuary continuum revealed by continuous observation [J]. *Journal of Geophysical Research: Biogeosciences*, 2022, **127**(8), doi: 10.1029/2022JG006786.
- [36] Yang B, Lin H, Bartlett S L, *et al.* Partitioning and transformation of organic and inorganic phosphorus among dissolved, colloidal and particulate phases in a hypereutrophic freshwater estuary [J]. *Water Research*, 2021, **196**, doi: 10.1016/j.watres.2021.117025.
- [37] Yao W S, Millero F J. Adsorption of phosphate on manganese dioxide in seawater [J]. *Environmental Science & Technology*, 1996, **30**(2): 536-541.
- [38] Dick W A, Tabatabai M A. Determination of orthophosphate in aqueous solutions containing labile organic and inorganic phosphorus compounds [J]. *Journal of Environmental Quality*, 1977, **6**(1): 82-85.
- [39] 延子轩, 冯民权. 长河流域矿区地表水水化学特征及驱动因子分析[J]. *环境化学*, 2022, **41**(2): 632-642.
Yan Z X, Feng M Q. Hydrochemical characteristics and driving factors of surface water in the mining area of Changhe River Basin [J]. *Environmental Chemistry*, 2022, **41**(2): 632-642.
- [40] 逢勇, 李学灵. 珠江三角洲河网入伶仃洋污染物通量计算研究[J]. *水利学报*, 2001, (9): 40-44.
Jiang Y, Li X L. Pollutant effluent flowing from the four eastern outlets of Pearl River Delta into Lingdingyang Sea [J]. *Journal of Hydraulic Engineering*, 2001, (9): 40-44.
- [41] 莫文渊, 韦惺, 吴超羽. 全新世以来珠江三角洲海鸟沙形成过程的地貌动力学分析[J]. *热带海洋学报*, 2019, **38**(3): 68-78.
Mo W Y, Wei X, Wu C Y. Morphodynamic analysis of Haiou sandbody evolution in Pearl River delta since Holocene [J]. *Journal of Tropical Oceanography*, 2019, **38**(3): 68-78.
- [42] 韩冰, 王效科, 欧阳志云. 城市面源污染特征的分析[J]. *水资源保护*, 2005, **21**(2): 1-4.
Han B, Wang X K, Ouyang Z Y. Analysis on characteristics of urban non-point source pollution [J]. *Water Resources Protection*, 2005, **21**(2): 1-4.
- [43] Jin X, Zhang W Q, Li S M. Complex responses of suspended particulate matter in eutrophic river and its indicative function in river recovery process [J]. *Ecological Indicators*, 2020, **115**, doi: 10.1016/j.ecolind.2020.106397.
- [44] Ji N N, Liu Y, Wang S R, *et al.* Buffering effect of suspended particulate matter on phosphorus cycling during transport from rivers to lakes [J]. *Water Research*, 2022, **216**, doi: 10.1016/j.watres.2022.118350.
- [45] Zaman M I, Mustafa S, Khan S, *et al.* Effect of phosphate complexation on Cd²⁺ sorption by manganese dioxide (β -MnO₂) [J]. *Journal of Colloid and Interface Science*, 2009, **330**(1): 9-19.

CONTENTS

Prediction of Autumn Ozone Concentration in the Pearl River Delta Based on Machine Learning	CHEN Zhen, LIU Run, LUO Zheng, <i>et al.</i> (1)
Remote Sensing Model for Estimating Atmospheric PM _{2.5} Concentration in the Guangdong-Hong Kong-Macao Greater Bay Area	DAI Yuan-yuan, GONG Shao-qi, ZHANG Cun-jie, <i>et al.</i> (8)
Variation Characteristics of PM _{2.5} Pollution and Transport in Typical Transport Channel Cities in Winter	DAI Wu-jun, ZHOU Ying, WANG Xiao-qi, <i>et al.</i> (23)
Characteristics of Secondary Inorganic Ions in PM _{2.5} and Its Influencing Factors in Summer in Zhengzhou	HE Bing, YANG Jie-ru, XU Yi-fei, <i>et al.</i> (36)
Characteristics and Source Apportionment of Carbonaceous Aerosols in the Typical Urban Areas in Chongqing During Winter	PENG Chao, LI Zhen-liang, XIANG Ying, <i>et al.</i> (48)
Analysis of Influencing Factors of Ozone Pollution Difference Between Chengdu and Chongqing in August 2022	CHEN Mu-lan, LI Zhen-liang, PENG Chao, <i>et al.</i> (61)
Analysis of O ₃ Pollution Affected by a Succession of Three Landfall Typhoons in 2020 in Eastern China	HUA Cong, YOU Yuan, WANG Qian, <i>et al.</i> (71)
Characteristics and Source Apportionment of VOCs Initial Mixing Ratio in Beijing During Summer	ZHANG Bo-tao, JING Kuan, WANG Qin, <i>et al.</i> (81)
Review of Comprehensive Evaluation System of Vehicle Pollution and Carbon Synergistic Reduction	FAN Zhao-yang, TONG Hui, LIANG Xiao-yu, <i>et al.</i> (93)
Study of Peak Carbon Emission of a City in Yangtze River Delta Based on LEAP Model	YANG Feng, ZHANG Gui-chi, SUN Ji, <i>et al.</i> (104)
Driving Forces and Mitigation Potential of CO ₂ Emissions for Ship Transportation in Guangdong Province, China	WENG Shu-juan, LIU Ying-ying, TANG Feng, <i>et al.</i> (115)
Carbon Emission Characteristics and Influencing Factors of Typical Processes in Drinking Water Treatment Plant	ZHANG Xiang-yu, HU Jian-kun, MA Kai, <i>et al.</i> (123)
Distribution Characteristics of Arsenic in Drinking Water in China and Its Health Risk Based on Disability-adjusted Life Years	DOU Dian-cheng, QI Rong, XIAO Shu-min, <i>et al.</i> (131)
Spatiotemporal Occurrence of Organophosphate Esters in the Surface Water and Sediment of Taihu Lake and Relevant Risk Assessment	ZHANG Cheng-nuo, ZHONG Qin, LUAN Bo-wen, <i>et al.</i> (140)
Exposure Level and Risk Impact Assessment of Pesticides and Veterinary Drugs in Aquaculture Environment	ZHANG Kai-wen, ZHANG Hai-yan, KONG Cong, <i>et al.</i> (151)
Variation in Phosphorus Concentration and Flux at Zhutuo Section in the Yangtze River and Source Apportionment	LOU Bao-feng, XIE Wei-min, HUANG Bo, <i>et al.</i> (159)
“Load-Unload” Effect of Manganese Oxides on Phosphorus in Surface Water of the Pearl River Estuary	LI Rui, LIANG Zuo-bing, WU Qi-ru, <i>et al.</i> (173)
Factors Influencing the Variation in Phytoplankton Functional Groups in Fuchunjiang Reservoir	ZHANG Ping, WANG Wei, ZHU Meng-yuan, <i>et al.</i> (181)
Hydrochemical Characteristics and Formation Mechanism of Groundwater in the Western Region of Hepu Basin, Beihai City	CHEN Wen, WU Ya, ZHANG Hong-xin, <i>et al.</i> (194)
Controlling Factors of Groundwater Salinization and Pollution in the Oasis Zone of the Cherchen River Basin of Xinjiang	LI Jun, OUYANG Hong-tao, ZHOU Jin-long (207)
Spatial-temporal Evolution of Ecosystem Health and Its Influencing Factors in Beijing-Tianjin-Hebei Region	LI Kui-ming, WANG Xiao-yan, YAO Luo-lan (218)
Spatial and Temporal Evolution and Impact Factors Analysis of Ecosystem Service Value in the Liaohe River Delta over the Past 30 Years	WANG Geng, ZHANG Fu-rong (228)
Effects of Photovoltaic Power Station Construction on Terrestrial Environment: Retrospect and Prospect	TIAN Zheng-qing, ZHANG Yong, LIU Xiang, <i>et al.</i> (239)
Spatiotemporal Evolution and Quantitative Attribution Analysis of Vegetation NDVI in Greater Khingan Mountains Forest-Steppe Ecotone	SHI Song, LI Wen, QU Chen, <i>et al.</i> (248)
Spatio-temporal Variation in Net Primary Productivity of Different Vegetation Types and Its Influencing Factors Exploration in Southwest China	XU Yong, ZHENG Zhi-wei, MENG Yu-chi, <i>et al.</i> (262)
Impacts of Extreme Climate Events at Different Altitudinal Gradients on Vegetation NPP in Songhua River Basin	CUI Song, JIA Zhao-yang, GUO Liang, <i>et al.</i> (275)
Spatial and Temporal Evolution and Prediction of Carbon Storage in Kunming City Based on InVEST and CA-Markov Model	Paruke Wusimanjiang, AI Dong, FANG Yi-shu, <i>et al.</i> (287)
Spatial-Temporal Evolution and Prediction of Carbon Storage in Jiuquan City Ecosystem Based on PLUS-InVEST Model	SHI Jing, SHI Pei-ji, WANG Zi-yang, <i>et al.</i> (300)
Soil Carbon Pool Allocation Dynamics During Soil Development in the Lower Yangtze River Alluvial Plain	HU Dan-yang, ZHANG Huan, SU Bao-wei, <i>et al.</i> (314)
Spatial Distribution Patterns of Soil Organic Carbon in Karst Forests of the Lijiang River Basin and Its Driving Factors	SHEN Kai-hui, WEI Shi-guang, LI Lin, <i>et al.</i> (323)
Effect of Land Use on the Stability of Soil Organic Carbon in a Karst Region	CHEN Jian-qi, JIA Ya-nan, HE Qiu-fang, <i>et al.</i> (335)
Spatial Distribution Characteristics of Soil Carbon and Nitrogen in Citrus Orchards on the Slope of Purple Soil Hilly Area	LI Zi-yang, CHEN Lu, ZHAO Peng, <i>et al.</i> (343)
Effects of Experimental Nitrogen Deposition and Litter Manipulation on Soil Organic Components and Enzyme Activity of Latosol in Tropical Rubber Plantations	XUE Xin-xin, REN Chang-qi, LUO Xue-hua, <i>et al.</i> (354)
Analysis on Driving Factors, Reduction Potential, and Environmental Effect of Inorganic Fertilizer Input in Chongqing	LIANG Tao, ZHAO Jing-kun, LI Hong-mei, <i>et al.</i> (364)
Research Progress on Distribution, Transportation, and Control of Per- and Polyfluoroalkyl Substances in Chinese Soils	LIU Hao-ran, XING Jing-yi, REN Wen-jie (376)
Prediction of Spatial Distribution of Heavy Metals in Cultivated Soil Based on Multi-source Auxiliary Variables and Random Forest Model	XIE Xue-feng, GUO Wei-wei, PU Li-jie, <i>et al.</i> (386)
Health Risk Assessment and Priority Control Factors Analysis of Heavy Metals in Agricultural Soils Based on Source-oriented	MA Jie, GE Miao, WANG Sheng-lan, <i>et al.</i> (396)
Contamination Characteristics and Source Apportionment of Soil Heavy Metals in an Abandoned Pyrite Mining Area of Tongling City, China	LI Ru-zhong, LIU Yu-hao, HUANG Yan-huan, <i>et al.</i> (407)
Source Apportionment and Assessment of Heavy Metal Pollution in Surface Dust in the Main District Bus Stops of Tianshui City	LI Chun-yan, WANG Xin-min, WANG Hai, <i>et al.</i> (417)
Response of Cadmium in Soil-rice to Different Conditioners Based on Field Trials	TANG Le-bin, LIU Xin-cai, SONG Bo, <i>et al.</i> (429)
Regulation Effects of Humus Active Components on Soil Cadmium Availability and Critical Threshold for Rice Safety	HU Xiu-zhi, SONG Yi, WANG Tian-yu, <i>et al.</i> (439)
Using Biochar and Iron-calcium Material to Remediate Paddy Soil Contaminated by Cadmium and Arsenic	WU Qiu-chan, WU Ji-zi, ZHAO Ke-li, <i>et al.</i> (450)
Research Progress on Characteristics of Human Microplastic Pollution and Health Risks	MA Min-dong, ZHAO Yang-chen, ZHU Long, <i>et al.</i> (459)
Effects of Polystyrene Microplastics Combined with Cadmium Contamination on Soil Physicochemical Properties and Physiological Ecology of <i>Lactuca sativa</i>	NIU Jia-rui, ZOU Yong-jun, JIAN Min-fei, <i>et al.</i> (470)
Transcriptome Analysis of Plant Growth-promoting Bacteria Alleviating Microplastic and Heavy Metal Combined Pollution Stress in Sorghum	LIU Yong-qi, ZHAO Si-yu, REN Xue-min, <i>et al.</i> (480)
Effects of Microplastics on the Leaching of Nutrients and Cadmium from Soil	ZHAO Qun-fang, CHU Long-wei, DING Yuan-hong, <i>et al.</i> (489)
Effect of Microplastics and Phenanthrene on Soil Chemical Properties, Enzymatic Activities, and Microbial Communities	LIU Sha-sha, QIN Jian-qiao, WU Xian-ge (496)
Prediction of Soil Bacterial Community Structure and Function in Minqin Desert-oasis Ecotone Artificial <i>Haloxylon ammodendron</i> Forest	WANG An-lin, MA Rui, MA Yan-jun, <i>et al.</i> (508)
Response of Soil Fungal Community to Biochar Application Under Different Irrigation Water Salinity	ZHENG Zhi-yu, GUO Xiao-wen, MIN Wei (520)
Effects of Organic Fertilizer of Kitchen Waste on Soil Microbial Activity and Function	LIU Mei-ling, WANG Yi-min, JIN Wen-hao, <i>et al.</i> (530)
Response Characteristics of Soil Fungal Community Structure to Long-term Continuous Cropping of Pepper	CHEN Fen, YU Gao, WANG Xie-feng, <i>et al.</i> (543)
Effects of Foliar Application of Silicon Fertilizers on Phyllosphere Bacterial Community and Functional Genes of Paddy Irrigated with Reclaimed Water	LIANG Sheng-xian, LIU Chun-cheng, HU Chao, <i>et al.</i> (555)
Analysis of Bacterial Communities and Antibiotic Resistance Genes in the Aquaculture Area of Changli County	WANG Qiu-shui, CHENG Bo, LIU Yue, <i>et al.</i> (567)
High-throughput qPCR and Amplicon Sequencing as Complementary Methods for Profiling Antibiotic Resistance Genes in Urban Wetland Parks	HUANG Fu-yi, ZHOU Shu-yi-dan, PAN Ting, <i>et al.</i> (576)
Characteristics of Vertical Distribution and Environmental Factors of Antibiotics in Quaternary Sedimentary Column in Urban Areas	LIU Ke, TONG Lei, GAN Cui, <i>et al.</i> (584)
Adsorption Performance and Mechanism of Oxytetracycline in Water by KOH Modified Biochar Derived from Corn Straw	LIU Zong-tang, SUN Yu-feng, FEI Zheng-hao, <i>et al.</i> (594)
Comparison of Pb ²⁺ Adsorption Properties of Biochars Modified Through CO ₂ Atmosphere Pyrolysis and Nitric Acid	JIANG Hao, CHEN Rui-zhi, ZHU Zi-yang, <i>et al.</i> (606)